Semnan University

Journal of Heat and Mass Transfer Research

Journal homepage: http://jhmtr.journals.semnan.ac.ir

2D Numerical Simulation of a Micro Scale Ranque-Hilsch Vortex Tube

Nader Rahbar[1,*], Mostafa Shateri[1], Mohsen Taherian[1], Mohammad Sadegh Valipour[2]

[1]*Department of Mechanical Engineering, Semnan Branch, Islamic Azad University, Semnan, Iran*
[2]*School of Mechanical Engineering, Semnan University, Semnan, Iran*

PAPER INFO

History:
Received 31 May 2014
Received in revised form 27 July 2014
Accepted 08 September 2014

Keywords:
Micro-Scale Vortex Tube
Energy separation
CFD Analysis
Refrigeration Capacity

A B S T R A C T

In this study, fluid flow and energy separation in a micro-scale Ranque-Hilsch Vortex Tube are numerically investigated. The flow is assumed as 2D, steady, compressible ideal gas, and shear-stress-transport $SST\ k-\omega$ is found to be a best choice for modeling of turbulence phenomena. The results are in a good agreement with the experimental results reported in the literature. The results show that fluid flow and energy separation inside the micro-scale vortex tube is quite similar to those of traditional ones. Moreover, it is found that non-dimensional forms of cold-temperature difference and refrigerating capacity are only dependent on cold mass fraction. In addition, two correlations have been proposed to estimate non-dimensional forms of cold temperature difference and refrigeration capacity in the micro-scale vortex tube.

1. Introduction

A Ranque-Hilsch Vortex Tube (RHVT) is a simple device without any moving parts. When a high-pressure gas is entered tangentially in a vortex tube, it is separated into two low-pressure hot and cold temperature streams. This phenomenon which is known as energy separation is first discovered by Ranque [1, 2] and after that it is developed by Hilsch [3].

To better understanding of the energy separation inside traditional RHVTs, several numerical investigations have been done during last decade. Fröhlingsdorf and Unger [4] numerically evaluated the fluid flow in a traditional RHVT. They used an axisymmetric 2-D model to evaluate the flow structure inside the RHVT. They identify a secondary circulating zone inside the vortex tube and conclude that this zone receives energy from a cold stream and transmits it to the hot gas. In a numerical and experimental study, Behera et al. [5] investigated the effect of different configuration of nozzles on energy separation in a traditional vortex tube. They report that for attaining a maximum cold temperature difference, the values of length to diameter ratio and non-dimensional orifice diameter should be $20< L/D<30$ and $dc/D=0.5$, respectively. Aljuwayhel et al. [6] studied the energy separation and flow structure in a RHVT by using Standard K-ε and RNG K-ε turbulence models. They concluded that RNG K-ε model provided better prediction than Standard K-ε model. In a similar study, Skye et al. [7] reported the opposite results of Aljuwayhel for simulating of a commercial vortex tube. In another numerical study, Eiamsa-ard and Promvonge [8]

Corresponding author: Nader Rahbar, School of Mechanical Engineering, Semnan Branch, Islamic Azad University, P.O. Box: 35196-97951, Semnan, Iran. *Email:*

simulated a uni-flow vortex tube. They used CFX commercial CFD code and axisymmetric 2-D model to simulate the energy separation inside the tube. Farouk and Farouk [9] reported that LES turbulence model was better than K-ε model for simulating of a vortex tube. Behera et al. [10] evaluated the effects of fluid flow properties, secondary circulation and tube length on the energy separation of a 3-D RHVT. They report that, in a large-scale vortex tube, the static temperature radially decreases near the entrance region.

In another study, Farouk et al. [11] simulated gas species and temperature separation inside a counter flow RHVT. They reported that, only a very minimal gas separation occurred inside the vortex tube as a result of diffusion effects. They also conclude that inner core flow has large values of eddy heat flux and Reynolds stresses.

Ameri and Behnia [12] used 2-D and 3-D RSM turbulence models to investigate the energy separation in a vortex tube. They find an optimum inlet-pressure for maximum efficiency. They also suggested the optimum dimensional values for their vortex tube. Dutta et al. [13] compare several different turbulence models and conclude that the value of hot and cold outlet temperatures obtained by the standard K-ε and SST K-ω models is very close to the experimental data. Hossein Nezhad and Shamsoddini [14] compared 2-D and 3-D numerical modeling of the flow stream in a vortex tube. They conclude that the results of a three-dimensional model are more accurate than 2-D one. Moreover, in another study Shamsoddini and Hossein Nejad [15]reportthat the number of nozzles has direct effect on the power of cooling and opposite effect on the cold outlet-temperature. Gas separation at atmospheric and cryogenic temperatures was numerically studied by Dutta et al. [16]. They reported an enhancement in predicting of the energy separation by using of NIST real gas model for accurately computing of the air properties. Baghdad et al. [17] investigated the energy separation mechanism and flow phenomena within a vortex tube by using four different turbulence models. They reported that advanced RSM model is the most accurate model to estimate cold and hot outlet temperatures. Khazaei et al. [18] reported that Spalart–Allmaras turbulence model has also good ability in estimating of flow field and energy separation in a typical vortex tube.

Typical vortex tubes have fairly large tube diameters (i.e. 10-25 mm) which limit their application specially in smal scale devices. A micro-scale vortex tube has a good potential for small-scale cooling applications such as cooling of electronic chips, cutter blades,plastic injection molds, and setting solders and adhesives. To the best knowledge of the authors of the present paper, there are not enough investigations on micro-scale vortex tubes. Dyskin and Kramarenko [19] were the first researchers that conducted some experimental procedures to determine the performance characteristics of a micro-scale vortex tube. Their vortex tube had an operating pressure ratio of 6 and diameters of 1 mm, 2 mm, and 3 mm. They reportthat, by decreasing of the flow- rate, the cooling effect decreases. Hamoudi et al. [20] experimentally investigated the performance of a micro-scale vortex tube. They conducted some experiments over a wide range of working pressure, different cold air mass ratio, different tube length, and orifice diameters. The results of their experiments at low Reynolds numbers show that by increasing of Reynolds number, dimensionless temperature increases in both hot and cold air flows. They also conclude that the optimum cold air mass fraction is not constant at high inlet pressure and it is higher than that of conventional vortex tubes. However, the effect of L/D and d_c/D ratios are similar to those of conventional devices. Rahbar et al. [21] numerically investigated the flow behavior and energy separation inside a micro-scale vortex tube. They show that both 2-D and 3-D CFD simulation have a good potential to estimate the performance of a micro-scale vortex tube. They also reported that in a micro-scale vortex tube, the expansion-effect on static temperature is more than that of large-scale vortex tubes.

The energy separation inside a micro-scale vortex tube is a significant phenomenon and all operational and performance characteristics are dependent on it. As mentioned before, there are few works to estimate flow characteristics of micro-scale vortex tubes. So, it requires more work to find insight of this process and to obtain some accurate correlations to estimate the performance of a micro-scale vortex tube. The aim of this work is to investigate the energy separation phenomenon and flow structure inside a 2-D micro-scale vortex tube by using of computational fluid dynamic. In addition, some correlations are proposed to estimate non-dimensional forms of cold temperature difference and refrigeration capacity in the micro-scale vortex tube.

2. Numerical Model Formulation

In this study, numerical analysis of the fluid regime in a micro-scale vortex tube is performed. Because of small size of inlet nozzles, it is essential to check the validation of continuum model in the micro-scale vortex tube. The continuum model is not valid, when the characteristic dimension is comparable with the mean free path of molecules. The ratio of the mean free path to the characteristic length, defines an important dimensionless parameter, called the Knudsen number, and it is given by [22, 23]:

$$Kn = \sqrt{\frac{\pi\gamma}{2}}\frac{M_{in}}{\mathrm{Re}_{in}}, \text{ where, } \mathrm{Re} = \frac{\dot{m}d_n}{4A\mu} \tag{1}$$

For values of $Kn \le 0.001$, the flow-regime is continuum. In the micro-scale vortex tube, the value of Knudsen number is equal to $Kn = 8.96\times10^{-5}$ at inlet nozzles and it is possible to apply Navier-Stokes and energy equations in the flow simulation.

In this study, the flow is assumed as steady, turbulent, compressible and, the governing equations for fluid flow and heat transfer are as follows [13]:

Continuity equation:

$$\frac{\partial}{\partial x_i}(\rho u_i) = 0 \tag{2}$$

Momentum equations:

$$\frac{\partial}{\partial x_j}(\rho u_i u_j) = -\frac{\partial P}{\partial x_i} + \frac{\partial}{\partial x_j}\left[2\mu S_{ij} - \frac{2}{3}\mu\delta_{ij}\frac{\partial u_i}{\partial x_i}\right] + \frac{\partial u_i}{\partial x_j}\left(-\overline{\rho u_i' u_j'}\right) \tag{3}$$

where

$$S_{ij} = \frac{1}{2}\left(\frac{\partial u_i}{\partial x_j} + \frac{\partial u_j}{\partial x_i}\right)$$

Energy equation:

$$\frac{\partial}{\partial x_i}\left(\rho u_i\left(h + \frac{1}{2}u_i u_j\right)\right) = \frac{\partial}{\partial x_j}\left[k_{eff}\frac{\partial T}{\partial x_j} + u_i(\tau_{ij})_{eff}\right] \tag{4}$$

$$, k_{eff} = K + \frac{c_p\mu_t}{\mathrm{Pr}_t}$$

State equation for an ideal gas:

$$P = \rho RT \tag{5}$$

The term of $-\overline{\rho u_i' u_j'}$ is called as Reynolds stress and must be modelled to close the Eq. (3). Boussinesq hypothesis is a common method for modelling of Reynolds stresses, and it is given as follows:

$$-\overline{\rho u_i' u_j'} = \mu_t\left(\frac{\partial u_i}{\partial x_j} + \frac{\partial u_j}{\partial x_i}\right) - \frac{2}{3}\left(\rho k + \mu_t\frac{\partial u_k}{\partial x_k}\right)\delta_{ij} \tag{6}$$

$$\tau_{eff} = \mu_{eff}\left(\frac{\partial u_j}{\partial x_i} + \frac{\partial u_i}{\partial x_j}\right) - \frac{2}{3}\mu_{eff}\frac{\partial u_k}{\partial x_k}\delta_{ij} \tag{7}$$

$$, \mu_{eff} = \mu_t + \mu$$

There are several models to calculate the turbulence viscosity, μ_t. In $k-\varepsilon$ turbulence model μ_t is calculated as a function of turbulent kinetic energy, k, and turbulence dissipation rate, ε. In $k-\omega$ turbulence model, μ_t is calculated as a function of turbulent kinetic energy, k, and specific dissipation rate, ω. There are also other RANS turbulence models such as *RNG* $k-\varepsilon$, $k-\varepsilon$ Realizable and *SST* $k-\omega$ discussed in more details in the literature [24].

The flow regime in a vortex tube is mainly classified into two categories: near-wall and central core regimes. The flow in central region has a higher level of turbulence and mixing, so using of $k-\omega$ turbulence model is preferred. On the other hand, as a result of viscosity effect, the flow near the walls has low velocity and turbulence, so $k-\omega$ turbulence model is the best choice for simulating of flow field near the walls. We show later that *SST* $k-\omega$ is the best choice for simulating of the turbulence regime in a micro-scale vortex tube. The shear-stress transport *SST* $k-\omega$, developed by Menter [25], effectively and accurately combines the formulation of $k-\omega$ and $k-\omega$ models by using a blending function. The blending function activates $k-\omega$ model near the wall, and $k-\omega$ model in the central region of the vortex tube. This modification improves the flow prediction with strong adverse pressure gradients and

separation[26]. In using of *SST* $k-\omega$, ω and k satisfy two following equations:

$$\frac{\partial}{\partial x_j}(\rho k u_i) = \frac{\partial}{\partial x_j}\left[\Gamma_k\left(\frac{\partial k}{\partial x_j}\right)\right] + \bar{G}_k - Y_k + S_k \quad (8)$$

$$\frac{\partial}{\partial x_j}(\rho \omega u_i) = \frac{\partial}{\partial x_j}\left[\Gamma_\omega\left(\frac{\partial k}{\partial x_j}\right)\right] + G_\omega + D_\omega - Y_\omega + S_\omega \quad (9)$$

More details about terms of μ_t , Γ_k , S_k , $\bar{G}_k$, Γ_ω , G_ω , D_ω , Y_ω and S_ω , can be found in the work of Cebeci [24].

3. Theoretical Background

In order to evaluate the performance of a micro-scale vortex-tube, some operational parameters should be calculated which are as follows:

Total temperature difference:

$$\Delta T_{hc} = T_h - T_c \quad (10)$$

Cold air temperature difference:

$$\Delta T_c = T_{in} - T_c \quad (11)$$

Non-dimensional Cold air temperature:

$$T_c^* = \frac{\Delta T_c}{T_{in}} \quad (12)$$

Refrigeration Capacity:

$$\dot{Q}_c = \dot{m}_c C_p \Delta T_c \quad (13)$$

Isentropic Efficiency:

$$\eta_{is} = \frac{\Delta T_c}{\Delta T_{cs}} \quad (14)$$

Isentropic temperature difference:

$$\Delta T_{cs} = T_{in} - T_{cs} = T_{in}\left[1 - \left(\frac{P_{atm}}{P_{in}}\right)^{(\gamma-1)/\gamma}\right] \quad (15)$$

Cold mass ratio:

$$y_c = \frac{\dot{m}_c}{\dot{m}_{in}} \quad (16)$$

4. Solution Procedures

In this study, the experimental report of Hamoudi et al. [20] was used to validate the numerical results. As shown in Fig. 1, to investigate the flow structure and energy separation phenomena, an axisymmetric two dimensional micro-scale vortex tube was simulated by using Fluent 6.3.26 software. The inlet nozzle was modelled as a continuous annular opening with a cross-sectional area equal to the total area of four inlet nozzles of the vortex tube reported in the study of Hamoudi et al. [20]. Moreover, the diameter of the cold outlet is chosen so that its area is the same as the cold-outlet area of 3-D RHVT. Table 1 shows the other dimensions of 2-D geometry. The boundary conditions are as follows:

- Mass flow inlet and static temperature were used at the inlets. Moreover, the angle between radial velocity component and resultant velocity is considered as 16.62^{O}C.
- Pressure-outlet boundary conditions were used for both hot and cold outlets. However, for cold-outlet its value was equal to atmospheric pressure and, the value of hot-outlet was varied to control the hot-outlet mass fraction [5, 15].
- Adiabatic and no-slip boundary conditions were considered on walls.

In fluent 6.3.26, governing equations of fluid flow are solved by finite-volume method. For convection-diffusion formulation, PRESTO was used as a pressure interpolation scheme and second-order upwind was used for others. The pressure-velocity coupling was also handled by

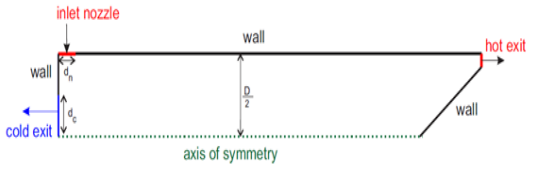

Fig. 1. Geometry of the micro-scale vortex tube used in 2-D simulation

Table 1. Dimensions of the micro-scale vortex tubes used for CFD modelling

	L (mm)	D (mm)	d_c (mm)	d_n (mm)
2-D simulation	20	2	0.55	0.141

using of SIMPLE algorithm (Semi Implicit Method for Pressure Linked Equations), described by Patankar [27, 28]. Air is also considered as an ideal gas with constant specific heat and variable viscosity and thermal conductivity. The solution is considered to be fully converged when the values of scaled-residuals from iteration to iteration are smaller than a prescribed value, 10^{-7} for energy equation and 10^{-5} for others.

Grid dependency tests have been done for all configurations investigated. The grid independency is attained when the percent changes of total temperature difference and tangential velocity are smaller than a given accuracy value 1%. Total number of nodal point is 14675. Figure 2 shows grid-dependency plots for 2-D micro-scale vortex tube, while Fig. 3 shows typical grids used for the CFD simulation.

5. Results and Discussions

To find the best turbulence model to simulate the micro-scale vortex tube, the results of five RANS turbulence models, standard $k-\varepsilon$, $RNG\ k-\varepsilon$, $k-\varepsilon$ Realizable, $k-\omega$ and $SST\ k-\omega$ are compared with experimental results of Hamoudi et al. [20]. Table 2 shows deviations of these models from experimental results. Moreover, the prediction of cold and hot outlet temperatures by different turbulence models are shown in Fig. 4 and Fig. 5. It is concluded that $SST\ k-\omega$ and

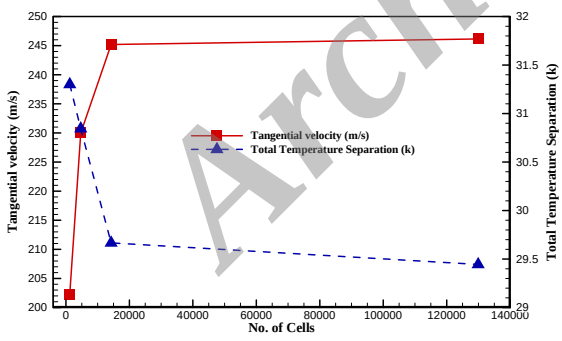

Fig. 2. Grid dependency check for 2-D micro-scale vortex tube

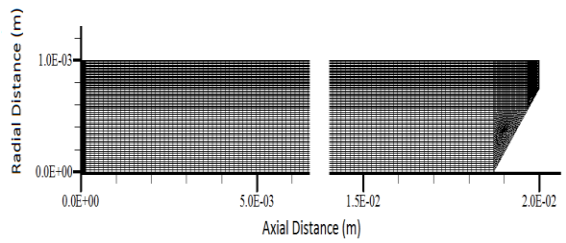

Fig. 3. Typical two-dimensional grid

$k-\omega$ are the best choices for prediction of cold outlet temperature and optimum cold-mass ratio. On the other hand, in spite of very good behaviour of $RNG\ k-\varepsilon$ and $k-\varepsilon$ Realizable, $SST\ k-\omega$ and $k-\omega$ have also good agreement with experimental results in prediction of hot-outlet temperature. As a result, in this study, $SST\ k-\omega$ is chosen for CFD-simulation of flow behaviours in a micro-scale vortex tube.

Variations of non-dimensional cold temperature, refrigeration capacity and isentropic efficiency versus cold mass ratio for different inlet pressures and non-dimensional tube length (L^*) are shown in Figs. 6-11. It can be concluded that the numerical simulation has a reasonable agreement with experimental results. However, CFD simulation over-predicts the values of non-dimensional cold temperature and refrigeration capacity. Moreover, the results show that optimum. values of T_c^*, refrigeration capacity and isentropic efficiency are achieved at $y_c = 0.58$, $y_c = 0.65$ and $y_c = 0.55$, respectively. These results are in accordance with experimental results of Skye et al. [7], and Valipour and Niazi [29] for a typical vortex-tube

Table 2. Deviations of different turbulence models from experimental results

Model	Deviation from experimental results		
	Cold-Outlet Temperature	Hot-Outlet Temperature	Optimum cold mass ratio
standard $k-\varepsilon$	3.2%	8%	2%
$RNG\ k-\varepsilon$	2.46%	1.41%	-55%
$k-\varepsilon$ Realizable	2.16%	1.76%	-55.5%
$k-\omega$	1.86%	4.4%	0.9%
$SST\ k-\omega$	1.84%	4%	0.5%

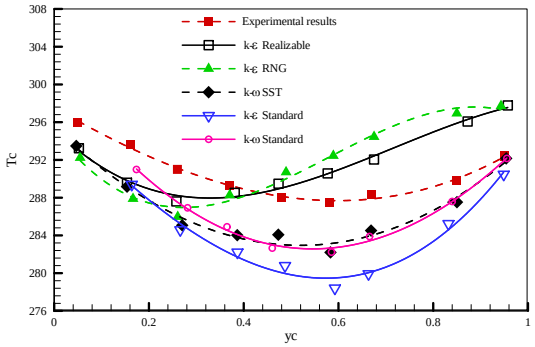

Fig. 4. Comparison between different turbulence models in prediction of cold-outlet temperature

$d_c^* = 0.55,\ L^* = 50$

Figures 12 -13 show the variation of non-dimensional cold temperature difference, $\Delta T_c/\Delta T_{c,\max}$, and refrigeration capacity, $\dot{Q}_C/\dot{Q}_{C,\max}$, versus cold mass fraction for different values of non-dimensional length and inlet pressure. It is observed that they are independent of geometry and inlet pressure (for both experimental and CFD results) and they are only a function of cold mass ratio.

Figures 14-15 show flow streamlines and contour of static temperature for cold mass ratios of 0.37 and 0.05, respectively. It is concluded that in a micro-scale RHVT, the back flow area for low values of cold mass flow rates is similar to that of conventional vortex tube reported by Skye et al. [7].

The numerical and experimental results of Figs. 12-13 can be correlated as polynomials by the best fit of data as follows:

$$\left.\frac{\Delta T_C}{\Delta T_{C,\max}}\right|_{\text{Experimental}} = -3.7491\times y_c^{\,2} + 4.1758\times y_c - 0.1924,\ R^2 = 0.96 \quad (17)$$

$$\left.\frac{\Delta T_C}{\Delta T_{C,\max}}\right|_{\text{Numerical}} = -3.6388\times y_c^{\,2} + 3.7496\times y_c + 0.0123,\ R^2 = 0.95 \quad (18)$$

$$\left.\frac{\dot{Q}_C}{\dot{Q}_{C,\max}}\right|_{\text{Experimental}} = -6.8336\times y_c^{\,3} + 7.8514\times y_c^{\,2} - 0.7568\times y_c + 0.0242,\ R^2 = 0.986 \quad (19)$$

$$\left.\frac{\dot{Q}_C}{\dot{Q}_{C,\max}}\right|_{\text{Numerical}} = -6.603\times y_c^{\,3} + 7.0161\times y_c^{\,2} - 0.3081\times y_c + 0.0159,\ R^2 = 0.97 \quad (20)$$

Variation of tangential velocity along radial-direction for different cross sections of the micro-

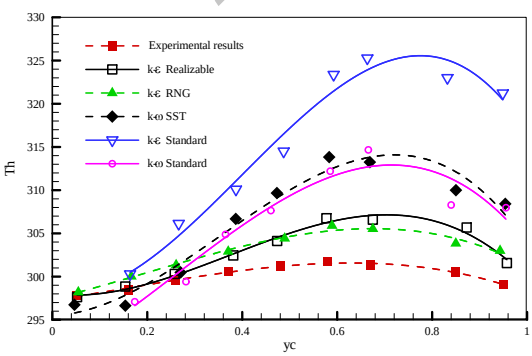

Fig. 5. Comparison between different turbulence models in prediction of hot-outlet temperature $d_c^* = 0.55,\ L^* = 50$

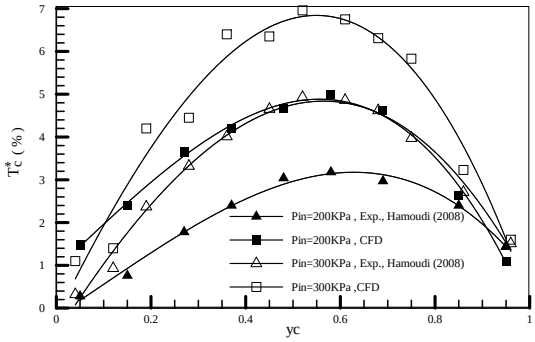

Fig. 6. Variation of non-dimensional cold temperature versus different cold mass ratio, $d_c^* = 0.55,\ L^* = 50$

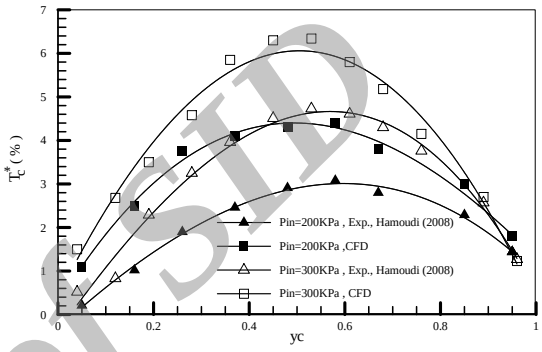

Fig. 7. Variation of non-dimensional cold temperature versus different cold mass ratio, $d_c^* = 0.55,\ L^* = 30$

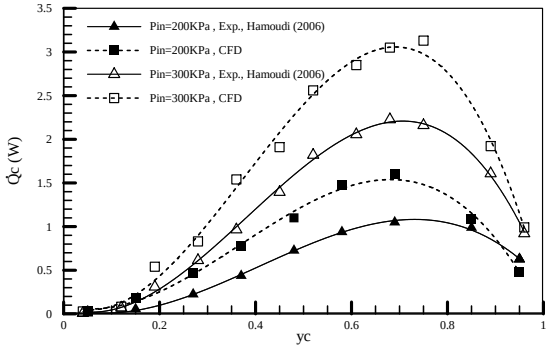

Fig. 8. Variation of Refrigeration Capacity versus different cold mass ratio, $d_c^* = 0.55,\ L^* = 50$

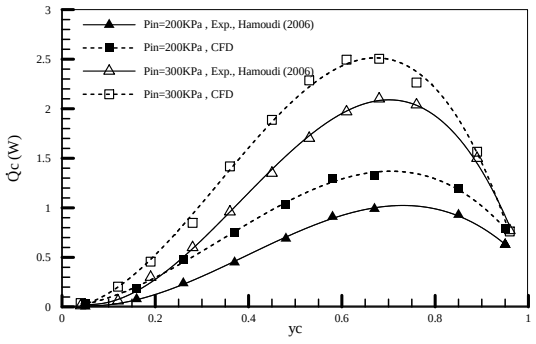

Fig. 9. Variation of Refrigeration Capacity versus different cold mass ratio, $d_c^* = 0.55,\ L^* = 30$

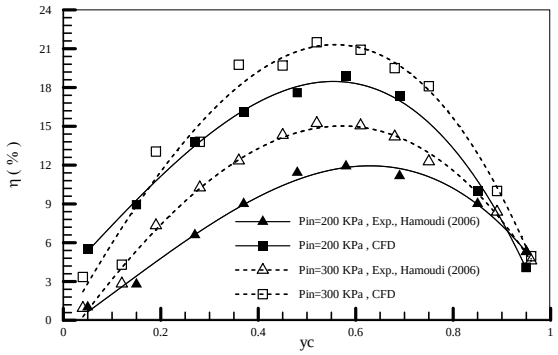

Fig. 10 – Variation of isentropic efficiency versus different cold mass ratio,

$d_c^* = 0.55,\ L^* = 50$

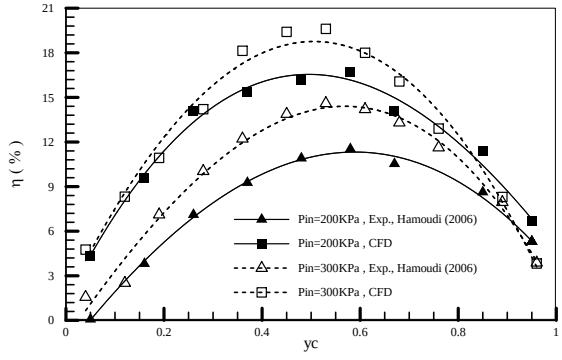

Fig. 11. Variation of isentropic efficienc yversus different cold mass ratio, $d_c^* = 0.55,\ L^* = 30$

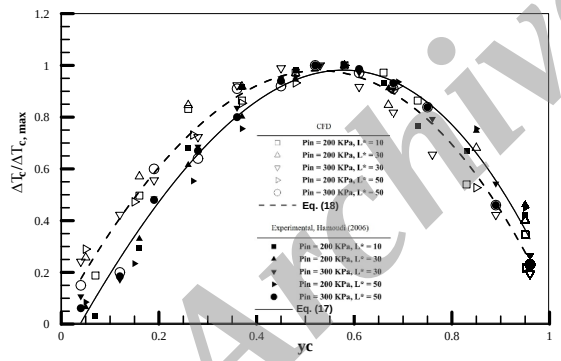

Fig. 12. Non-dimensional cold temperature difference versus cold mass ratio

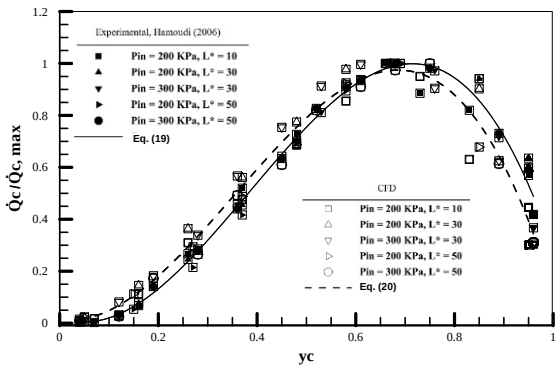

Fig. 13. Non-dimensional Refrigeration Capacity versus cold mass ratio

scale vortex tube is shown in Fig. 16. It is concluded that tangential velocity is maximum in the vicinity of inlet-zone. When the fluid moves helically toward the hot exit, the tangential velocity decreases alongside the vortex tube as a result of wall friction and friction between the fluid layers [10].

Variation of axial velocity along radial direction is shown in Fig. 17. The axial velocity is zero near $r = 0.73R$, which is the separating-line between hot

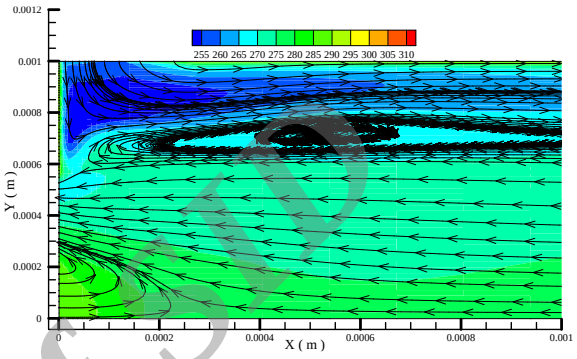

Fig. 14. Streamlines with back flow region and the distribution of static temperature,

$y_c = 0.37,\ L = 20mm, D = 2mm,\ d_c = 1.1mm,\ P_{in} = 200Kpa$

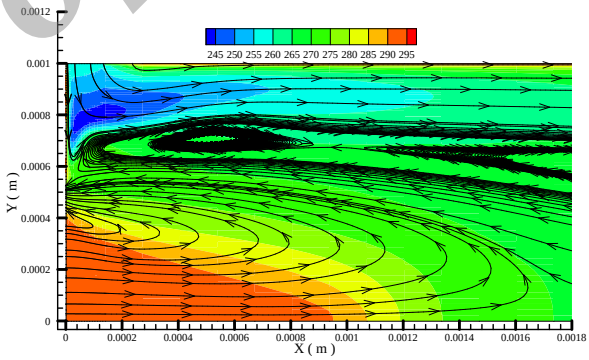

Fig. 15. Streamlines with back flow region and the distribution of static temperature,

$y_c = 0.05,\ L = 20mm, D = 2mm,\ d_c = 1.1mm,\ P_{in} = 200Kpa$

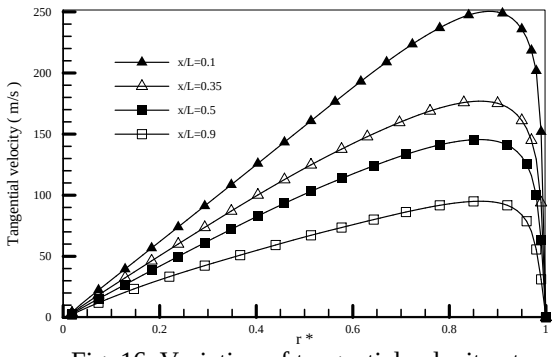

Fig. 16. Variation of tangential velocity at different cross sections of micro RHVT,

$y_c = 0.05,\ L = 20mm, D = 2mm,\ d_c = 1.1mm,\ P_{in} = 200Kpa$

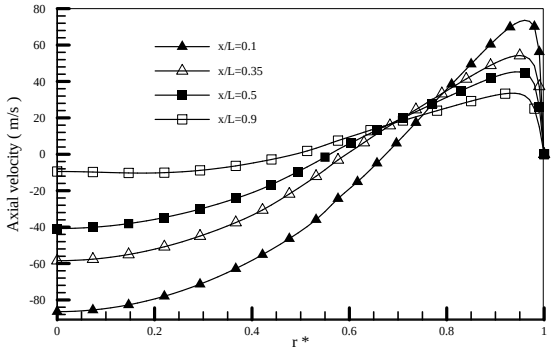

Fig. 17. Variation of axial velocity at different cross sections of micro RHVT,
$y_c = 0.05,\ L = 20mm, D = 2mm,\ d_c = 1.1mm,\ P_{in} = 200Kpa$

and cold streams. For the values of $r > 0.73R$, the direction of flow is toward the hot-outlet, and for the values of $r < 0.73R$, its direction is toward the cold-outlet.

Distribution of static pressure along radial direction for different cross-sections of the tube is shown in Fig. 18. The results show that for values of $r < 0.73R$, the static pressure increases by moving from inlet nozzles toward hot-outlet. This means that there exists a flowing stream from hot-outlet to cold-outlet in the central part of the tube. However, for the values of $r > 0.73R$, the static pressure decreases along axial direction and the direction of flow is toward hot-outlet. Moreover, it is observed that the static pressure is constant on the separating-line between hot and cold streams.

Fig. 19 shows streamlines inside the micro-scale RHVT. It is indicated that there exist a free vortex near the wall and forced vortex in the central region.

Distribution of static temperature as a function of radius, along the micro-scale vortex tube is shown in Fig. 20. It is concluded that the static temperature increases from inlet section toward hot

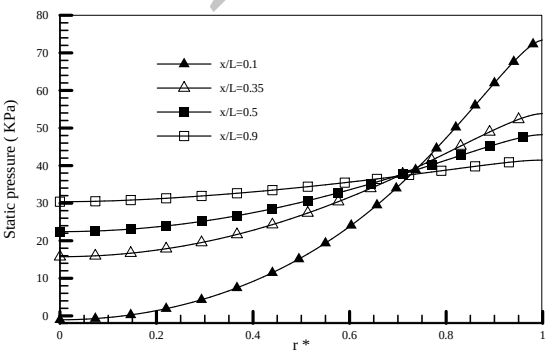

Fig. 18. Variation of static pressure at different cross sections of micro RHVT,
$y_c = 0.05,\ L = 20mm, D = 2mm,\ d_c = 1.1mm,\ P_{in} = 200Kpa$

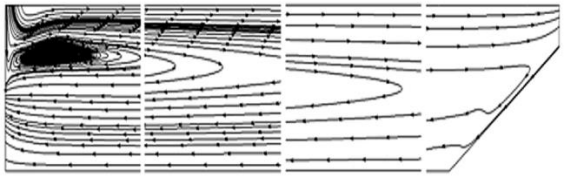

Fig. 19 – Streamlines of flow inside the micro-scale vortex tube,
$y_c = 0.05,\ L = 20mm, D = 2mm,\ d_c = 1.1mm,\ P_{in} = 200Kpa$

exit as a result of decreasing of tangential velocity due to friction.

Moreover, it is observed that, except the entrance region, the static temperature is radially constant in the central-zone of the micro-scale vortex tube. Contours of total temperature are shown in Fig. 21. The separation of energy inside the micro-scale RHVT in radial and axial direction can be seen in this figure.

6. Conclusion

In this study, energy separation phenomenon inside a micro-scale vortex tube was investigated by using of computational fluid dynamic. For this purpose, a 2-D axisymmetric model in Fluent 6.3.26 software has been used and its results have been compared with the experimental results reported in the literature. The main results obtained may be summarized as follows:

- The numerical results are in a good agreement with experimental data.
- Turbulence model of $SST\ k-\omega$ has been proposed for CFD-estimation of flow behavior in a micro-scale vortex tube.
- By analyzing the distribution of axial velocity, tangential velocity, static pressure, static temperature and total temperature inside the micro-scale RHVT, it can be concluded that

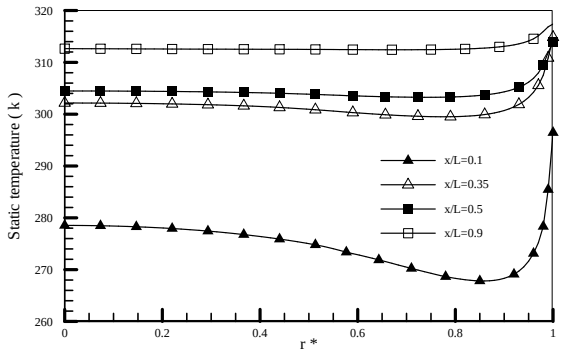

Fig. 20. Radial distribution of static temperature at different cross sections,
$y_c = 0.05,\ L = 20mm, D = 2mm,\ d_c = 1.1mm,\ P_{in} = 200Kpa$

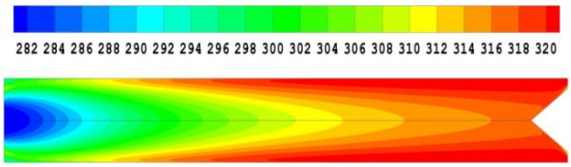

Fig. 21. Contour of total temperature (*K*) inside the micro-scale vortex tube, $y_c = 0.53$

the mechanism of energy separation and flow field are similar to those of conventional vortex tube reported in the literature.

- It is found that variations of non-dimensional cold temperature difference, $\Delta T_c/\Delta T_{c,\max}$, and refrigeration capacity, $\dot{Q}_C/\dot{Q}_{C,\max}$, are only dependent on cold mass fraction. Moreover, some relations have been proposed to estimate those parameters.

Acknowledgments

This work was supported by the Office of the Vice Chancellor for Research, Islamic Azad University, Semnan Branch, with Grant No.1108 - 21/05/1389. The authors would like to express their grateful thanks to Islamic Azad University, Semnan Branch, for providing information, experimental facilities and their close cooperation.

Nomenclature

A	*Area, m^2*
c_p	*Specific heat at constant Pressure, $Jkg^{-1}K^{-1}$*
d_n , D	*Diameter,m*
d_c^*	*Non-dimensional orifice diameter, (dc/D)*
E	*Total energy,Jkg^{-1}*
h	*Mass average enthalpy, Jkg^{-1}*
k	*Turbulence kinetic energy, m^2s^{-2}*
K	*Thermal conductivity,$Wm^{-1}K^{-1}$*
Kn	*Knudsen number*
L	*Length, m*
L^*	*Non-dimensional tube length to the diameter ratio, (L/D)*
M	*Mach number*
$\dot{m}$	*Mass flow rate, kgs^{-1}*
P	*Pressure, Pa*
Pr	*Prandtle number*
$\dot{Q}_c$	*Refrigeration capacity,W*
r	*Change in tube radius along y, m*
r^*	*Non-dimensional radius (r/R)*
R	*Specific constant of an ideal gas, $Jkg^{-1}K^{-1}$*
Re	*Reynolds number*
T	*Temperature, K*
u	*Mass averaged velocity, ms^{-1}*
u'	*Fluctuating velocity component, ms^{-1}*
x	*Axial distance from cold exit, m*
y	*Radial distance from tube axis, m*
y_c	*Cold mass fraction*

Greek symbols

δ_{ij}	*Kronecker delta*
γ	*Specific heat ratio, c_p/c_v*
μ	*Viscosity, $N.s.m^{-2}$*
μ_t	*Eddy viscosity, $N.s.m^{-2}$*
υ	*Kinematics viscosity, $m^2.s^{-1}$*
ρ	*Density,$kg.m^{-3}$*
τ	*Stress tensor*
ω	*Specific dissipation rate*
η_{is}	*Isentropic efficiency*
$(\tau_{ij})_{eff}$	*Stress tensor*

Subscripts

a	*Atmospheric*
c	*Cold exit*
cs	*Isentropic*
eff	*Effective*
h	*Hot exit*
in	*Inlet*
is	*Isentropic*
I, j, k	*Cartesian indices*
t	*Turbulent*
o	*Overall*

References

[1]. Ranque G. Experiments on expansion in a vortex with simultaneous exhaust of hot air and cold air. Le Journal de Physique et le Radium (Paris). 1933;4:112-4.

[2]. Ranque G. Method and apparatus for obtaining from a fluid under pressure two outputs of fluid at different temperatures. US1934.

[3]. Hilsch R. The use of the expansion of gases in a centrifugal field as cooling process. Review of Scientific Instruments. 1947;18(2):108-13.

[4]. Fröhlingsdorf W, Unger H. Numerical investigations of the compressible flow and the energy separation in the Ranque-Hilsch vortex tube. International Journal of Heat and Mass Transfer. 1999;42(3):415-22.

[5]. Behera U, Paul PJ, Kasthurirengan S, Karunanithi R, Ram SN, Dinesh K, et al. CFD analysis and experimental investigations towards optimizing the parameters of Ranque-Hilsch vortex tube. International Journal of Heat and Mass Transfer. 2005;48(10):1961-73.

[6]. Aljuwayhel NF, Nellis GF, Klein SA. Parametric and internal study of the vortex tube using a CFD model. International Journal of Refrigeration. 2005;28(3):442-50.

[7]. Skye HM, Nellis GF, Klein SA. Comparison of CFD analysis to empirical data in a commercial

vortex tube. International Journal of Refrigeration. 2006;29(1):71-80.
[8]. Eiamsa-ard S, Promvonge P. Numerical investigation of the thermal separation in a Ranque-Hilsch vortex tube. International Journal of Heat and Mass Transfer. 2007;50(5-6):821-32.
[9]. Farouk T, Farouk B. Large eddy simulations of the flow field and temperature separation in the Ranque-Hilsch vortex tube. International Journal of Heat and Mass Transfer. 2007;50(23-24):4724-35.
[10]. Behera U, Paul PJ, Dinesh K, Jacob S. Numerical investigations on flow behaviour and energy separation in Ranque-Hilsch vortex tube. International Journal of Heat and Mass Transfer. 2008;51(25-26):6077-89.
[11]. Farouk T, Farouk B, Gutsol A. Simulation of gas species and temperature separation in the counter-flow Ranque-Hilsch vortex tube using the large eddy simulation technique. International Journal of Heat and Mass Transfer. 2009;52(13-14):3320-33.
[12]. Ameri M, Behnia B. The study of key design parameters effects on the vortex tube performance. Journal of Thermal Science. 2009;18(4):370-6.
[13]. Dutta T, Sinhamahapatra KP, Bandyopdhyay SS. Comparison of different turbulence models in predicting the temperature separation in a Ranque-Hilsch vortex tube. International Journal of Refrigeration. 2010;33(4):783-92.
[14]. Nezhad AH, Shamsoddini R. Numerical three-dimensional analysis of the mechanism of flow and heat transfer in a vortex tube. Thermal Science. 2009;13(4):183-96.
[15]. Shamsoddini R, Nezhad AH. Numerical analysis of the effects of nozzles number on the flow and power of cooling of a vortex tube. International Journal of Refrigeration. 2010;33(4):774-82.
[16]. Dutta T, Sinhamahapatra K, Bandyopadhyay S. Numerical investigation of gas species and energy separation in the Ranque-Hilsch vortex tube using real gas model. International Journal of Refrigeration. 2011.
[17]. Baghdad M, Ouadha A, Imine O, Addad Y. Numerical study of energy separation in a vortex tube with different RANS models. International Journal of Thermal Sciences. 2011;50(12):2377-85.
[18]. Khazaei H, Teymourtash A, Jafarian M. Effects of gas properties and geometrical parameters on performance of a vortex tube. Scientia Iranica B. 2012;19(3):454-62.
[19]. Dyskin L, Kramarenko P. Energy characteristics of vortex microtubes. Journal of Engineering Physics and Thermophysics. 1984;47(6):1394-5.
[20]. Hamoudi A, Fartaj A, Rankin G. Performance Characteristics of a Microscale Ranque–Hilsch Vortex Tube. Journal of Fluids Engineering. 2008;130:101206.
[21]. Rahbar N, taherian M, Shateri M, valipour MS. Numerical investigation on flow behavior and energy separation in a micro-scale vortex tube. Thermal Science. 2012.
[22]. Hamoudi AF. An Investigation of a Micro-Scale Ranque-Hilsch Vortex Tube: University of Windsor,Windsor, ON, Canada, 2006.
[23]. Zhang Z. Nano/microscale heat transfer. 1st ed: McGraw-Hill Professional, 2007.
[24]. Cebeci T. Turbulence models and their application: efficient numerical methods with computer programs: Horizons Pub. and Springer, 2004.
[25]. Menter FR. Two-equation eddy-viscosity turbulence models for engineering applications. AIAA journal. 1994;32(8):1598-605.
[26]. Cebeci T. Analysis of turbulent flows. 2nd ed: Elsevier, 2004.
[27]. Patankar SV. Numerical heat transfer and fluid flow: Hemisphere Pub, 1980.
[28]. Versteeg HK, Malalasekera W. An introduction to computational fluid dynamics: the finite volume method: Prentice Hall, 2007.
[29]. Valipour MS, Niazi N. Experimental Modeling of a Curved Ranque-Hilsch Vortex Tube Refrigerator. International Journal of Refrigeration. 2011;34(4):1109–16.

شبیه سازی عددی دوبعدی یک لوله گردبادی در مقیاس میکرو

نادر رهبر[1،*]، مصطفی شاطری[1]، محسن طاهریان[1]، محمدصادق ولی‌پور[2]

۱. گروه مهندسی مکانیک، واحد سمنان، دانشگاه آزاد اسلامی، سمنان، ایران
۲. دانشکده مهندسی مکانیک، دانشگاه سمنان، سمنان

اطلاعات مقاله

دریافت مقاله: ۱۰خرداد ۱۳۹۳
پذیرش مقاله: ۸ شهریور ۱۳۹۳

واژگان کلیدی:
لوله گردبادی مقیاس میکرو،
جدایش انرژی،
تحلیل CFD،
ظرفیت تبرید،
.

چکیده

در این تحقیق جریان سیال و جدایش انرژی درون یک لوله گردبادی در مقیاس میکرو توسط دینامیک سیالات محاسباتی مورد بررسی قرار گرفته است. جریان سیال دو بعدی، پایدار، گازایده آل غیر قابل تراکم فرض شده و مدل توربولانسی SST K- ω به عنوان بهترین مدل در تحلیل جریان در این دستگاه تعیین شده است. نتایج حاصل از محاسبات عددی توافق خوبی را با نتایج آزمایشگاهی گزارش شده توسط سایر محققان نشان می دهند. نتایج نشان می دهند که رفتار سیال و جدایش انرژی درون لوله گردبادی میکرو شبیه رفتار سیال درون لوله های گردبادی متداول می باشند. علاوه بر آن مقادیر بی بعد اختلاف دمای سرد و ظرفیت تبرید تنها بستگی به مقدار کسر جرمی سرد دارند. همچنین در این تحقیق دو معادله جهت تخمین مقادیر بی بعد اختلاف دمای سرد و ظرفیت تبرید پیشنهاد گردیده است.